Supplementary Information

Solid-State Synthesis of few-layer Cobalt-doped MoS2 with CoMoS phase on Nitrogen-doped Graphene Driven by Microwave Irradiation

Junpeng Fan,[a] Joakim Ekspong,[a] Anumol Ashok,[b] Sergey Koroidov,[c] and Eduardo Gracia-Espino*[a]

[a] Department of Physics, Umeå University, Umeå 90187, Sweden

[b] Department of Materials and Environmental Chemistry, Stockholm University, Stockholm 106 91, Sweden.

[c] Department of Physics, Stockholm University, Stockholm 106 9, Sweden.

[*] Corresponding author: Eduardo Gracia-Espino (Email: eduardo.gracia@umu.se)

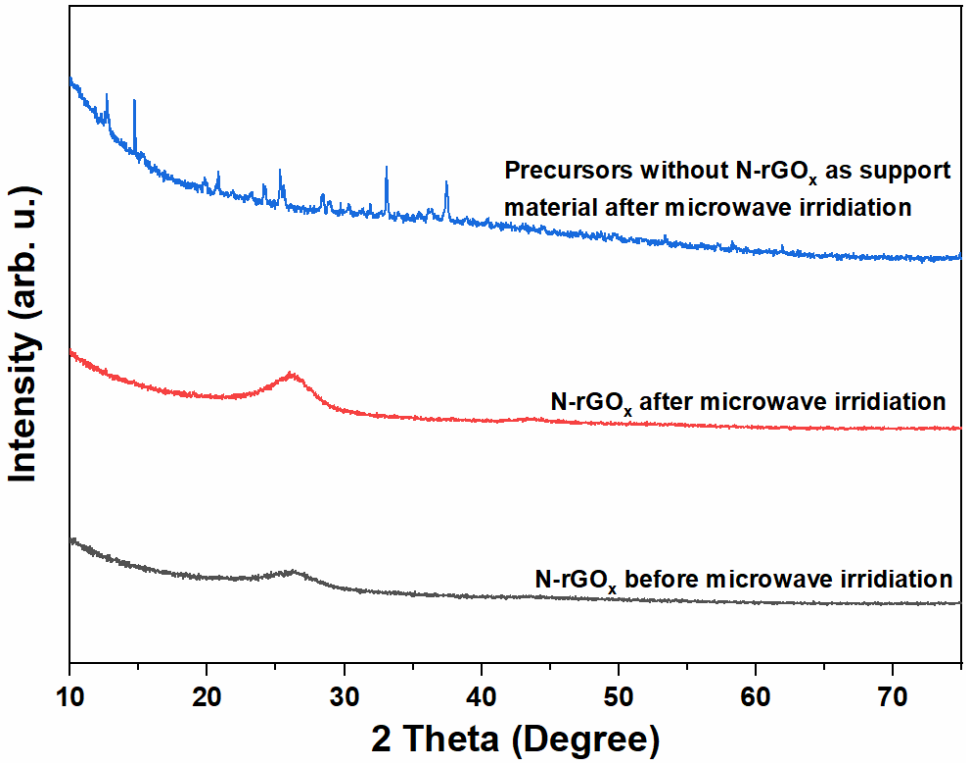

Fig. S1. XRD pattern of control samples.

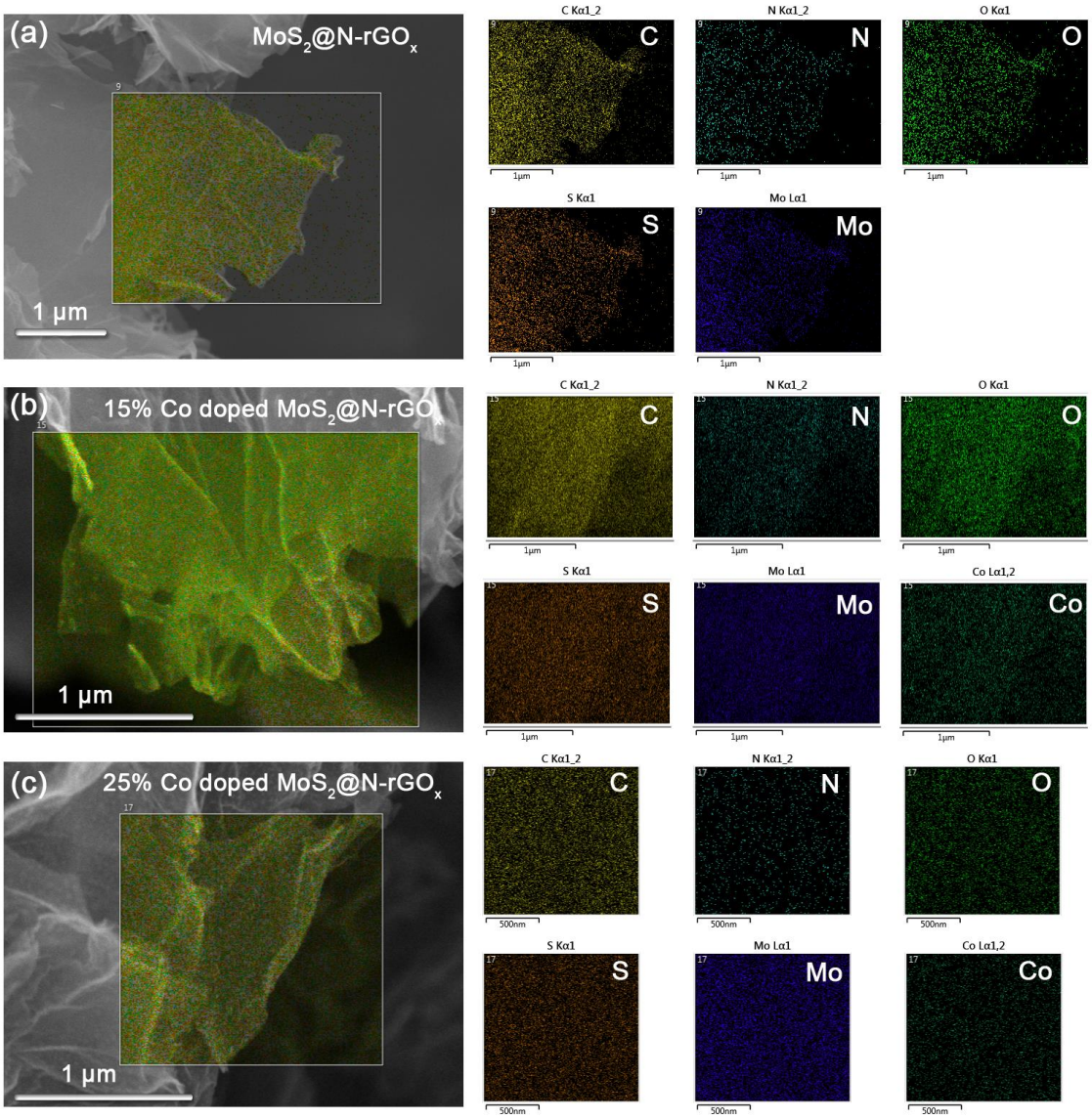

Fig. S2. SEM-EDS mapping and the corresponding element distribution of (a) MoS_2@N-rGO_x, (b) 15% Co-MoS_2@N-rGO_x and (c) 25% Co-MoS_2@N-rGO_x

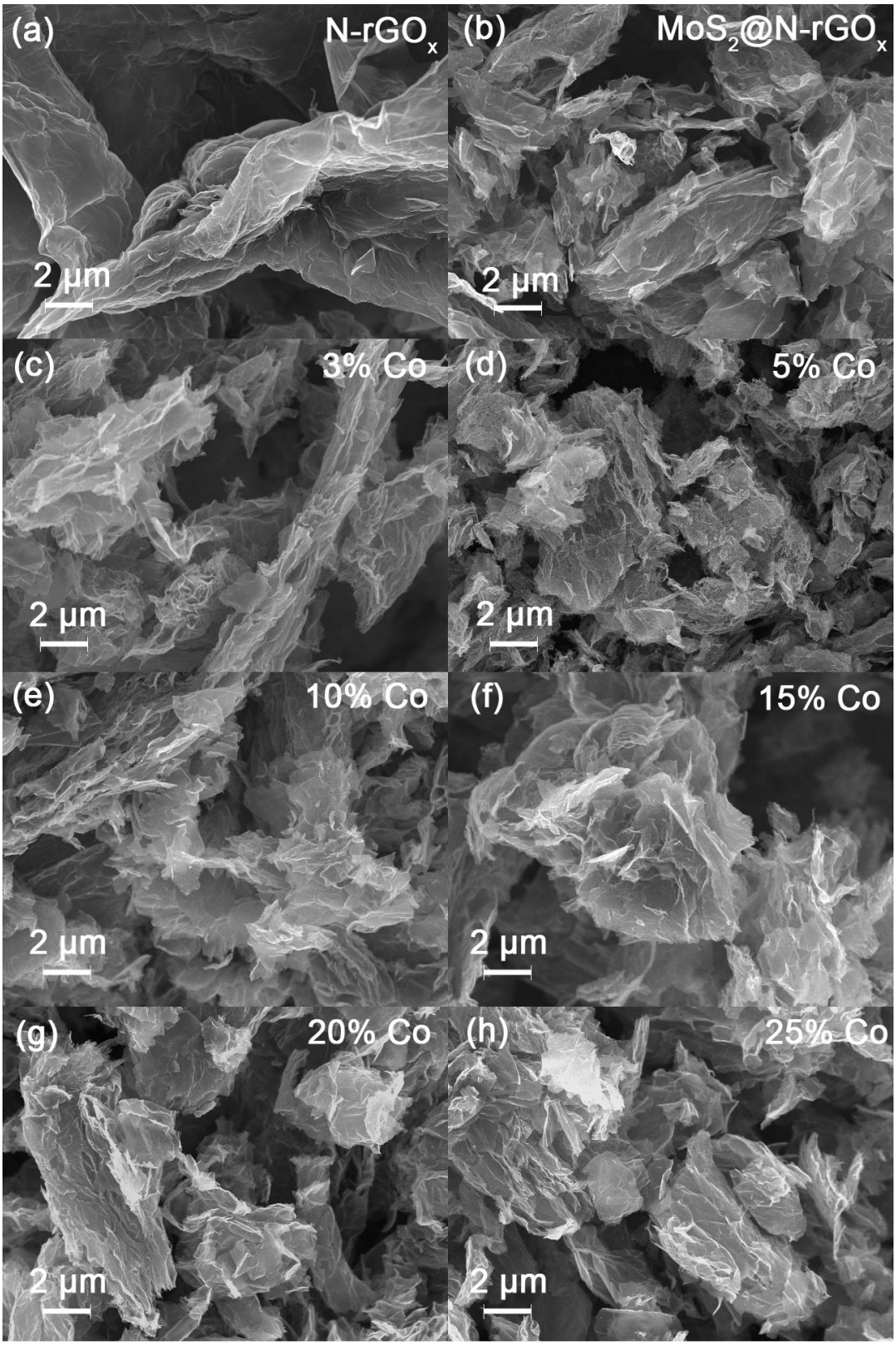

Fig. S3. (a)-(h) SEM images of N-rGO$_x$ and Co-MoS$_2$@N-rGO$_x$.

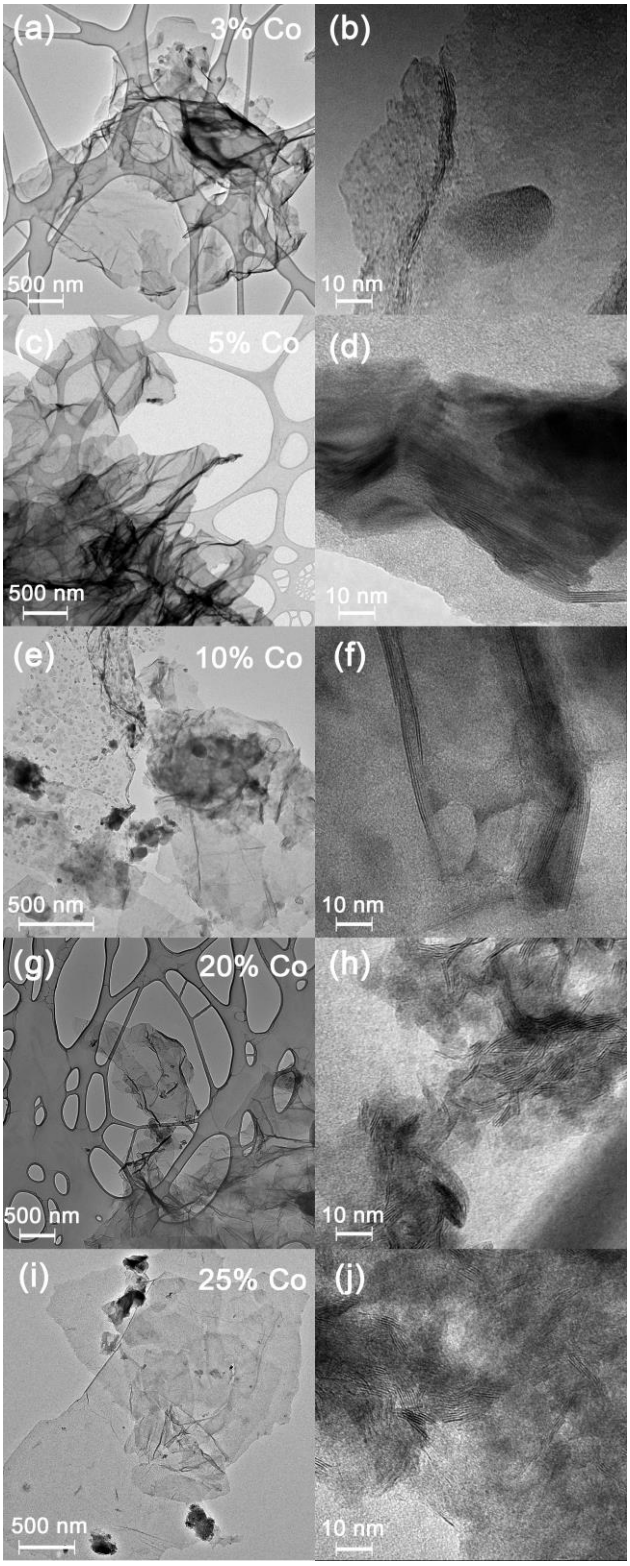

Fig. S4. TEM image of (a-b) 3%, (c-d) 5%, (e-f) 10%, (g-h) 20%, and (i-j) 25% Co-MoS_2@N-rGO_x.

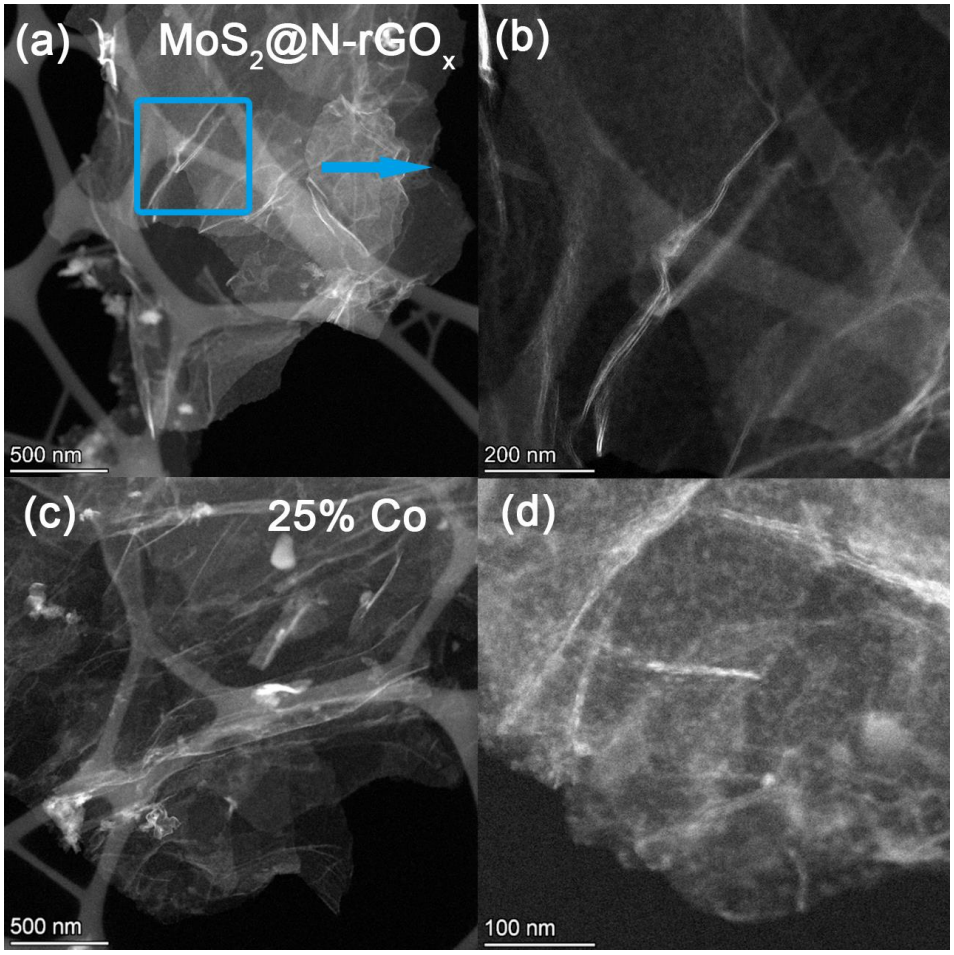

Fig. S5. STEM-HAADF images of (a-b) MoS_2@N-rGO_x, and (c-d) 25% Co-MoS_2@N-rGO_x.

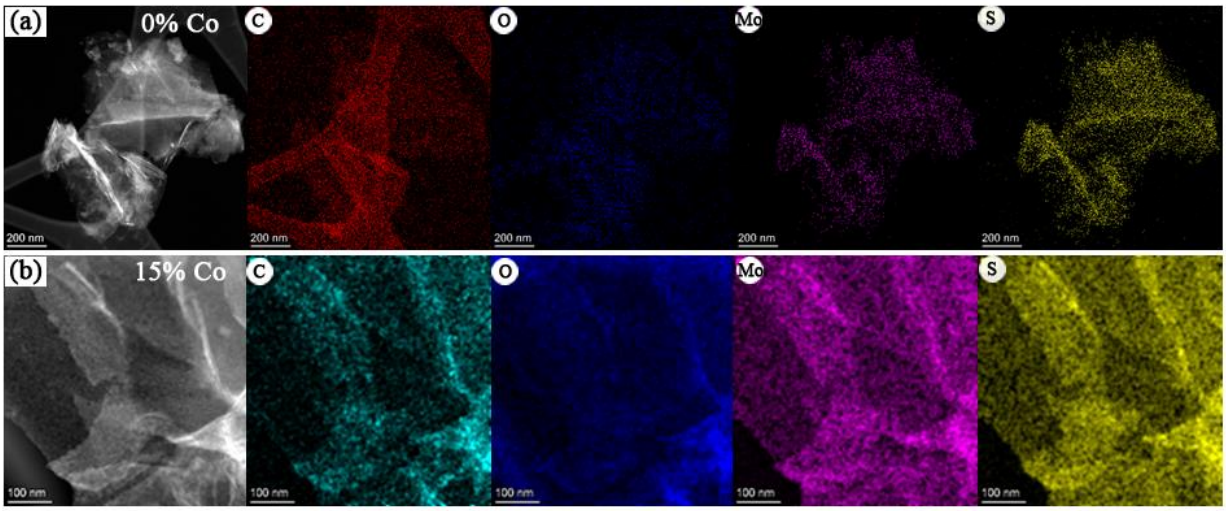

Fig. S6. Elemental mapping of (a) MoS_2@N-rGOx and (b) 15% Co-MoS_2@N-rGOx

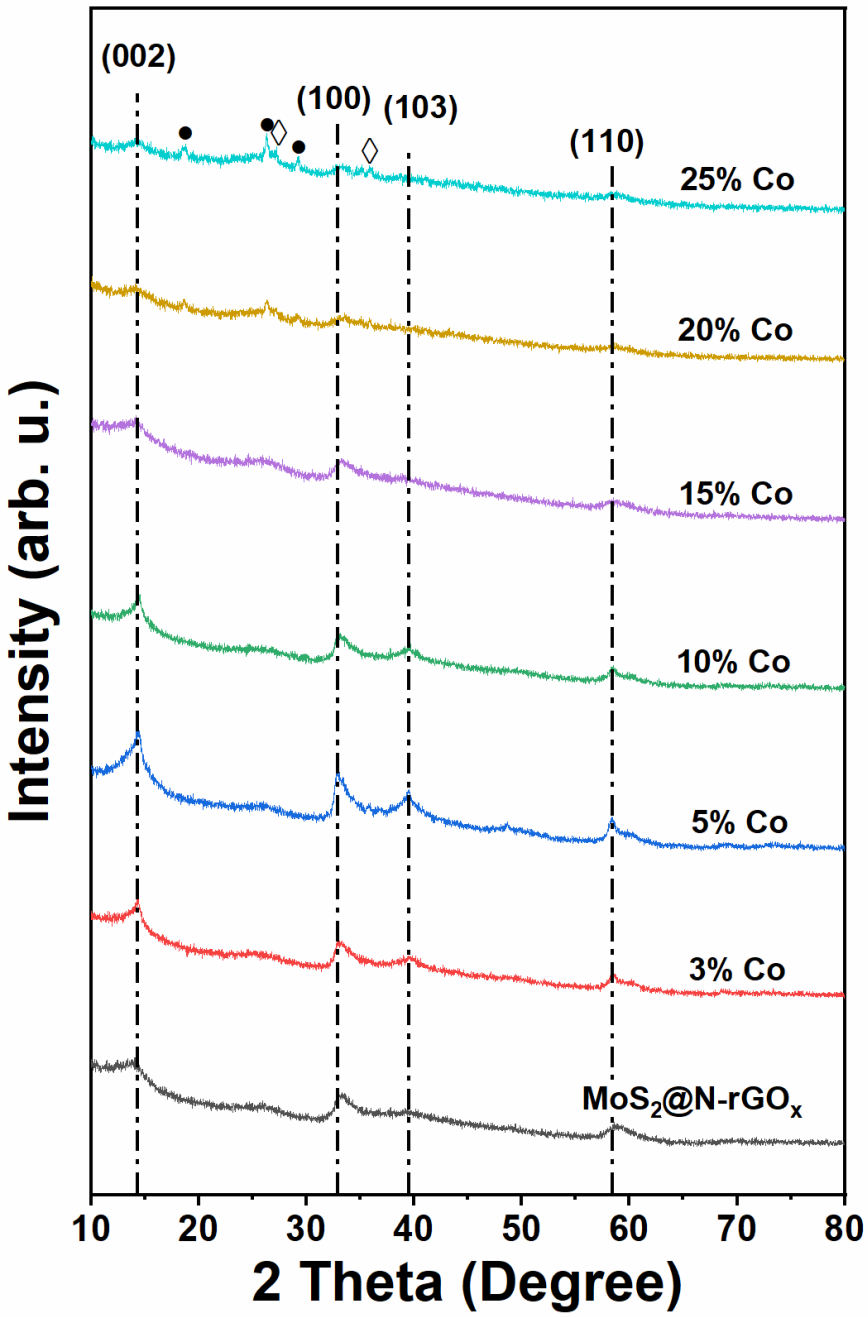

Fig. S7. XRD patterns of the synthesized samples after placing 3 months. Peaks marked by ● are associated with $CoMoS_{2.17}O_{1.12}$ and peaks marked by ◊ can be assigned to $CoMoS_{2.96}O_{0.25}$

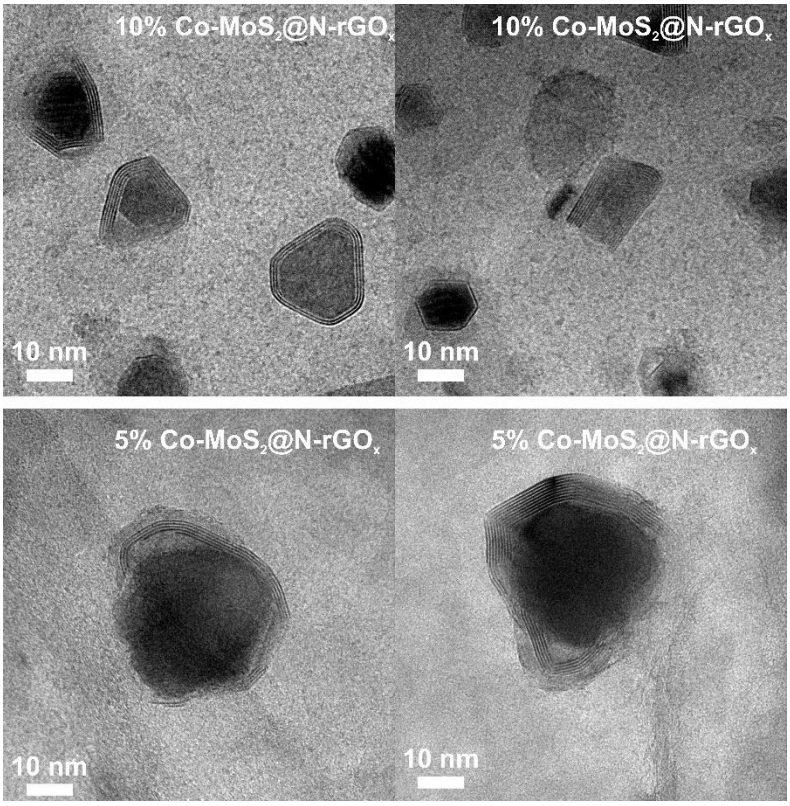

Fig. S8. Core-shell nanoparticles observed on 5% and 10%Co-MoS_2@N-rGO_x. The shell has an interlayer distance consistent with MoS_2.

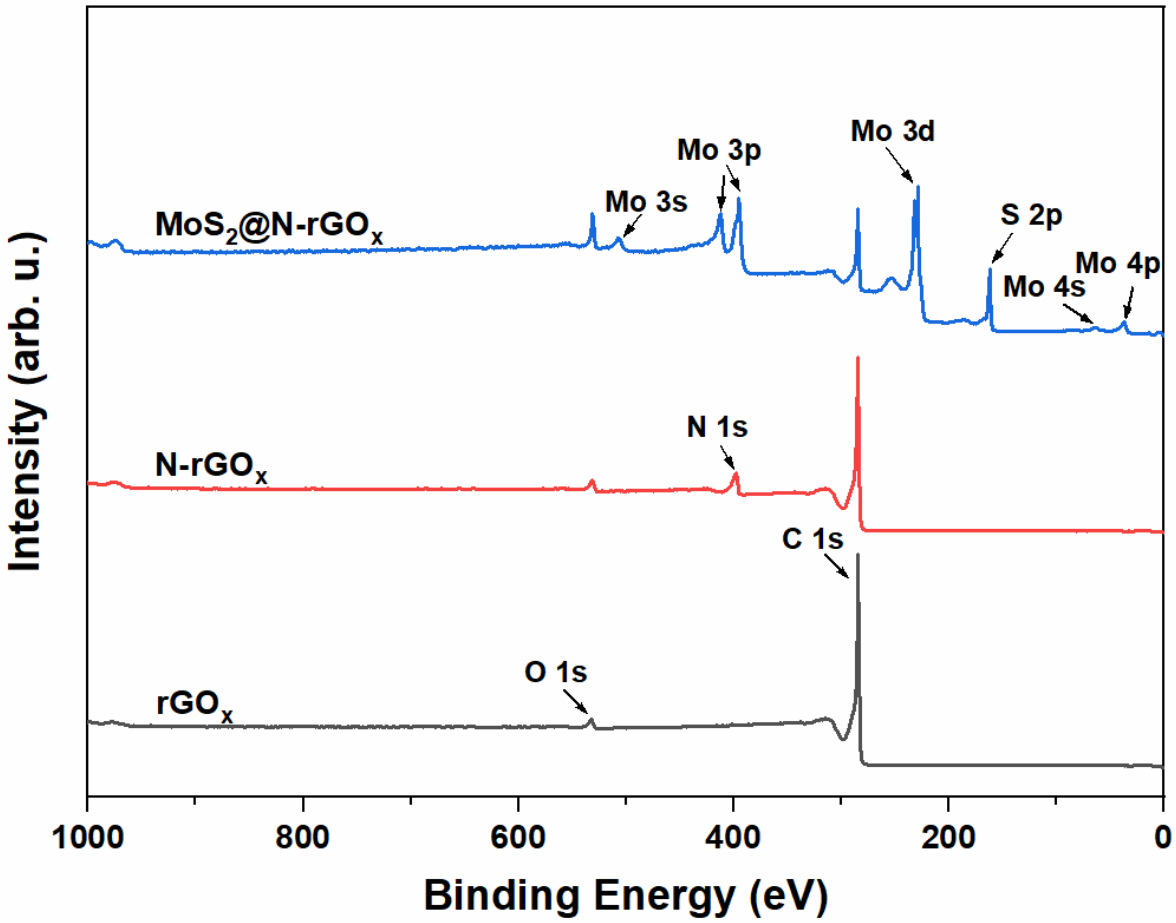

Fig. S9. Survey XPS spectra of pristine rGO_x, N-rGO_x and MoS_2@N-rGO_x. Note that in MoS_2@N-rGO_x the peak of Mo 3p overlaps with N 1s.

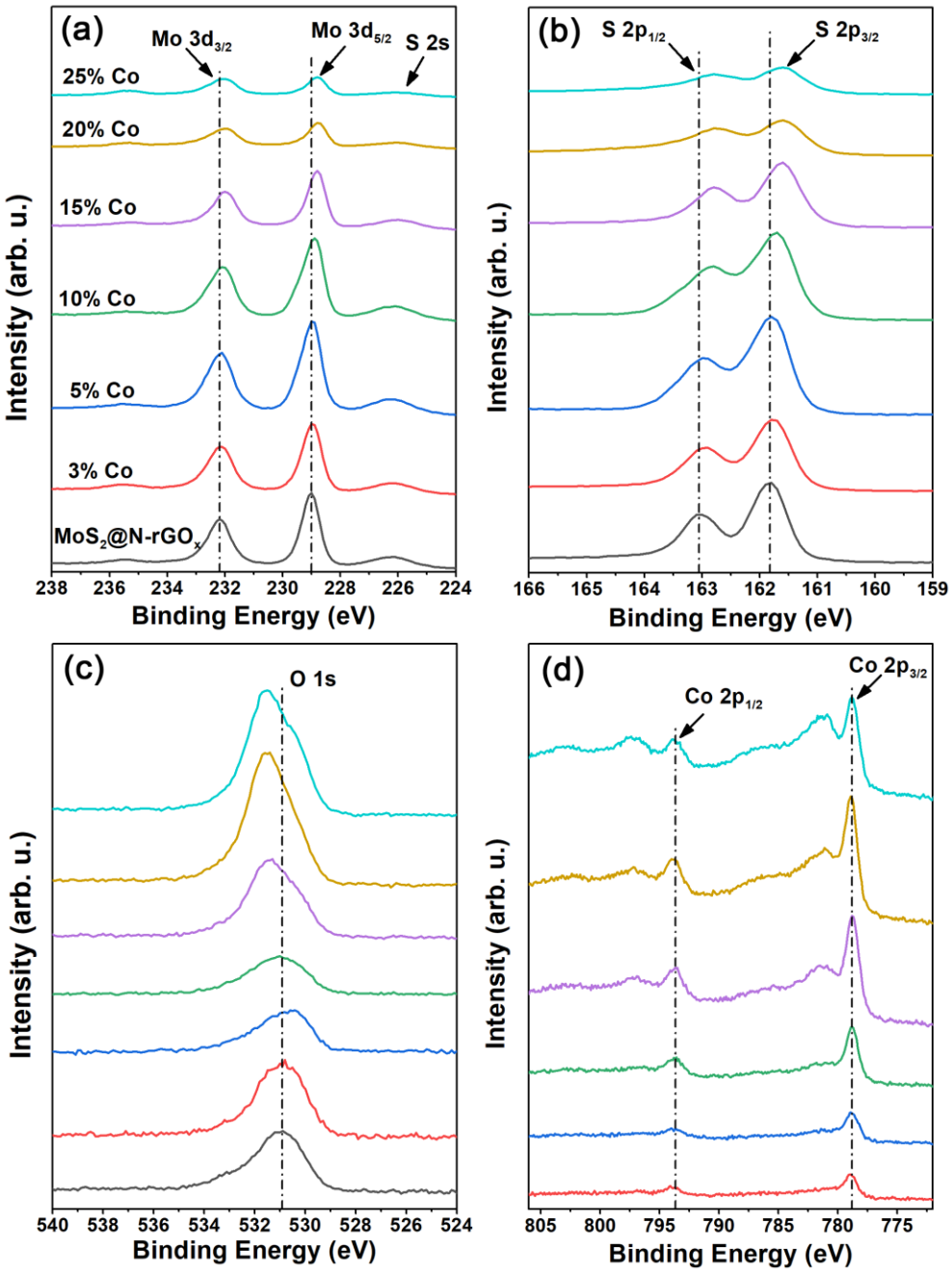

Fig. S10. XPS spectra evolution of (a) Mo 3d, (b) S 2p, (c) O 1s and (d) Co 2p peaks with Co doping.

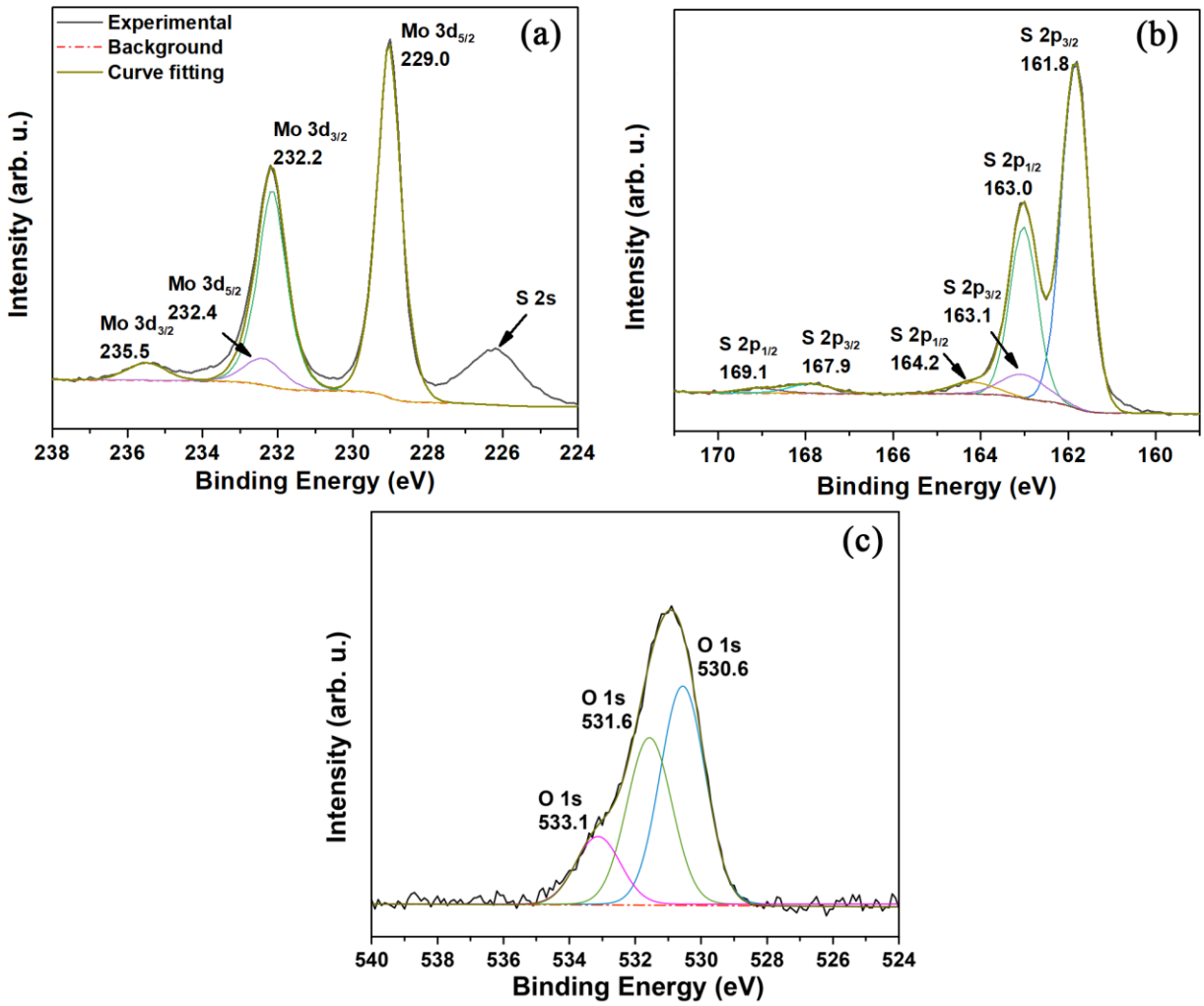

Fig. S11. XPS spectra deconvolution about (a) Mo 3d, (b) S 2p and (c) O 1s in the sample with MoS_2@N-rGO_x

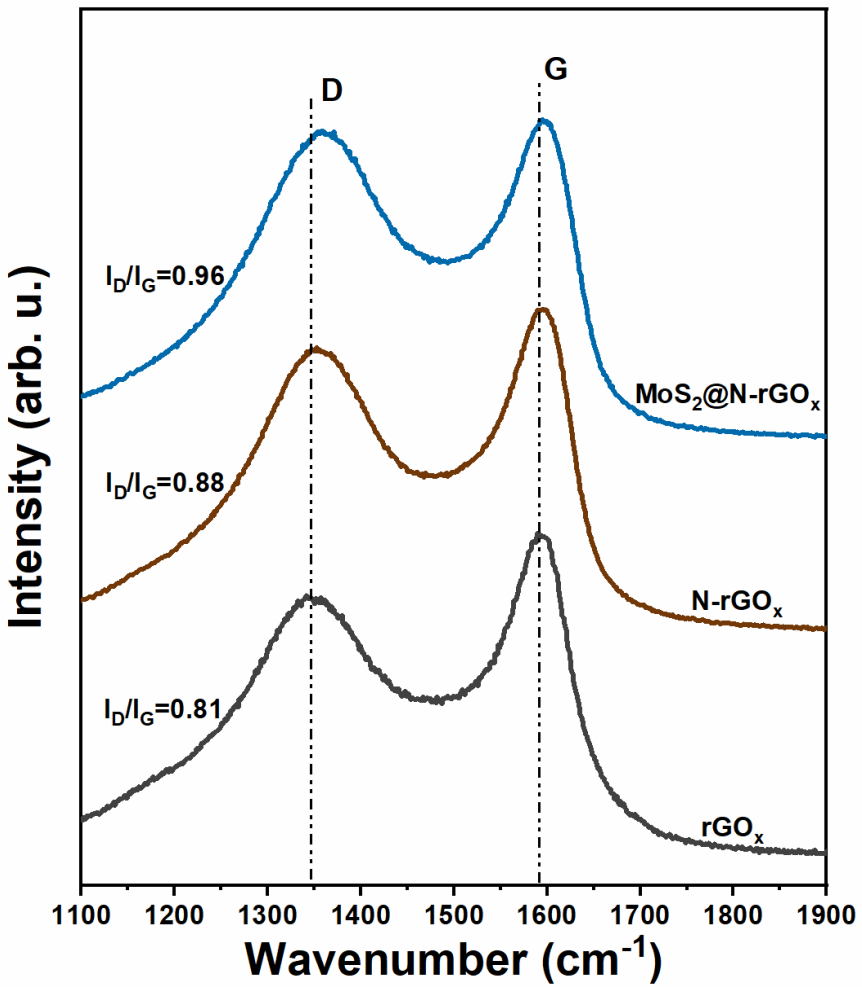

Fig. S12. Raman spectra of rGO_x, N-rGO_x and MoS_2@N-rGO_x.

Table S1 Atomic ratio of each element in the synthesized samples

(a) Detected by EDS

	C	N	O	S	Mo	Co	Others
N-rGO	91.45	5.55	2.95	-	-	-	
MoS_2@N-rGO$_x$	65.375	6.225	8.49	11.895	8.025	-	
3% Co doped MoS_2@N-rGO$_x$	57.63	7.44	14.95	11.74	7.675	0,57	
5% Co doped MoS_2@N-rGO$_x$	58.295	4.345	6.33	19,805	10.33	0.89	
10% Co doped MoS_2@N-rGO$_x$	66.11	4.845	9.63	12.245	5.825	1.34	
15% Co Doped MoS_2@N-rGO$_x$	64.035	5.615	10.735	11.865	5.315	2.33	Si 0.105
20% Co doped MoS_2@N-rGO$_x$	62,36	6.73	13.66	10.025	4.475	2.75	
25% Co doped MoS_2@N-rGO$_x$	64.82	7.34	14.265	7.305	3.21	3.06	

(b) Detected by XPS

	C	N	O	S	Mo	Co	Others
N-rGO	89.79	7.79	2.41	-	-	-	
MoS_2@N-rGO$_x$	64.41	-	8.09	17.6	9.9	-	
3% Co doped MoS_2@N-rGO$_x$	56.21	-	11.42	19.31	12.36	0.73	
5% Co doped MoS_2@N-rGO$_x$	52.55	-	5.87	25.03	14.92	1.02	
10% Co doped MoS_2@N-rGO$_x$	51.61	-	6.59	25.20	14.59	2.03	
15% Co Doped MoS_2@N-rGO$_x$	57.96	-	11.44	17.15	9.35	4.11	
20% Co doped MoS_2@N-rGO$_x$	55.32	13.96	12.85	10.08	3.92	3.87	
25% Co doped MoS_2@N-rGO$_x$	59.06	10.96	13.35	8.42	3.63	4.64	

Table S2 Comparison of HER activity of microwave synthesized 15% Co doped MoS_2@N-rGO with MoS_2 related catalysts described in published articles.

Catalysts	Synthesis method	Overpotential η at 10 mA·cm^{-2} (mV)	Tafel slope (mV·dec^{-1})	References
CoMoS	Co-precipitation followed annealing	135	50	1
2D MoS_2 monolayer	CVD followed hydrogen plasma treatment	183	77.6	2
CoS_2 nanowires	Solvothermal	145	51.6	3
MoS_2 on hydrogenated graphene	Solvothermal	124	41	4
1T´ MoS_2 on graphitic nanoribbons	Solvothermal	205	50	5
1T MoS_2	CVD followed *n*-Butyl lithium exfoliation	187	43	6
Co_9S_8@MoS_2 on CNFs	Electrospinning followed CVD	190	110	7
MoS_2-rGO_{240}	Microwaved assisted solvothermal	104	63	8
Ag_2S/MoS_2/rGO	Solvothermal	190	56	9
3D-Co-MoS_2 on graphene	Hard template and solvothermal	143	71	10
MoS_2 quantum dots	Pulsed laser ablation	~200	49	11
Amorphous MoS_x	Electrodeposition	160	-	12
MoS_2 on rGO	Modified hydrothermal	140	50	13
Rose-like MoS_2 and exfoliated WS_2 on carbon nanotube	Solvothermal	212	50	14
Co doped MoS_2 on N-rGO_x (as-synthesized)	Microwave irradiation	197	61	This work

Reference

1 X. Dai, K. Du, Z. Li, M. Liu, Y. Ma, H. Sun, X. Zhang and Y. Yang, *ACS Appl. Mater. Interfaces*, 2015, **7**, 27242–27253.

2 C. C. Cheng, A. Y. Lu, C. C. Tseng, X. Yang, M. N. Hedhili, M. C. Chen, K. H. Wei and L. J. Li, *Nano Energy*, 2016, **30**, 846–852.

3 M. S. Faber, R. Dziedzic, M. A. Lukowski, N. S. Kaiser, Q. Ding and S. Jin, *J. Am. Chem. Soc.*, 2014, **136**, 10053–10061.

4 X. Han, X. Tong, X. Liu, A. Chen, X. Wen, N. Yang and X. Y. Guo, *ACS Catal.*, 2018, **8**, 1828–1836.

5 J. Ekspong, R. Sandström, L. P. Rajukumar, M. Terrones, T. Wågberg and E. Gracia-Espino, *Adv. Funct. Mater.*, 2018, **28**, 1802744.

6 M. A. Lukowski, A. S. Daniel, F. Meng, A. Forticaux, L. Li and S. Jin, *J. Am. Chem. Soc.*, 2013, **135**, 10274–10277.

7 H. Zhu, J. Zhang, R. Yanzhang, M. Du, Q. Wang, G. Gao, J. Wu, G. Wu, M. Zhang, B. Liu, J. Yao and X. Zhang, *Adv. Mater.*, 2015, **27**, 4752–4759.

8 M. Chatti, T. Gengenbach, R. King, L. Spiccia and A. N. Simonov, *Chem. Mater.*, 2017, **29**, 3092–3099.

9 G. Solomon, R. Mazzaro, S. You, M. M. Natile, V. Morandi, I. Concina and A. Vomiero, *ACS Appl. Mater. Interfaces*, 2019, **11**, 22380–22389.

10 X. Meng, L. Yu, C. Ma, B. Nan, R. Si, Y. Tu, J. Deng, D. Deng and X. Bao, *Nano Energy*, 2019, **61**, 611–616.

11 J. Tang, M. Sakamoto, H. Ohta and K. Saitow, *Nanoscale*, 2020, **12**, 4352–4358.

12 O. Mabayoje, Y. Liu, M. Wang, A. Shoola, A. M. Ebrahim, A. I. Frenkel and C. B. Mullins, *ACS Appl. Mater. Interfaces*, 2019, **11**, 32879–32886.

13 T. Aditya, A. K. Nayak, D. Pradhan, A. Pal and T. Pal, *Electrochim. Acta*, 2019, **313**, 341–351.

14 P. Thangasamy, S. Oh, S. Nam and I.-K. Oh, *Carbon*, 2020, **158**, 216–225.